Robotica (2007) volume 25, pp. 189–199. © 2007 Cambridge University Press
doi:10.1017/S0263574707003384 Printed in the United Kingdom

# Sensor-based global planning for mobile robot navigation

S. Garrido†, L. Moreno†,*, D. Blanco† and M. L. Munoz‡

†*Carlos III University, Avd. de la Universidad, 30 28911, Leganés, Madrid, Spain*
‡*Facultad de Informática, Universidad Politécnica de Madrid, 28660 Boadilla del Monte, Madrid, Spain*

(Received in Final Form: January 5, 2007)

**SUMMARY**
The proposed algorithm integrates in a single planner the global motion planning and local obstacle avoidance capabilities. It efficiently guides the robot in a dynamic environment. This eliminates some of the traditional problems of planned architectures (model-plan-act scheme) while obtaining many of the qualities of behavior-based architectures. The computational efficiency of the method allows the planner to operate at high-rate sensor frequencies. This avoids the need for using both a collision-avoidance algorithm and a global motion planner for navigation in a cluttered environment. The method combines map-based and sensor-based planning operations to provide a smooth and reliable motion plan. Operating on a simple grid-based world model, the method uses a fast marching technique to determine a motion plan on a Voronoi extended transform extracted from the environment model. In addition to this real-time response ability, the method produces smooth and safe robot trajectories.

KEYWORD: Sensor-based global path planner; Fast marching; mobile robots; mobile manipulators.

## 1. Introduction

Robot motion planning problems have been an important research topic that has received more attention since the 1980s. A wide range of researchers have been working extensively to obtain efficient methods to solve these problems. This problem has been focused on in two general ways: one approach has concentrated on solving motion-planning problems by considering a previously known global environment and obstacles information and robot characteristics, and a second approach has focused on planning motions by using local sensor information and the robot characteristics.

The first approach has been used extensively at a global planning level in robotics to plan trajectories from one environment point to another. This plan obviously will only work under the assumption of a perfectly controlled and modeled environment, which does not exist in most situations. Unexpected obstacles, persons or moving elements make it difficult to use except in tightly controlled environments such as in industrial manipulation environments (manufacturing).

The second approach becomes evident in mobile robotics from the very beginning. Mobile robot environments present unexpected objects which make it impossible to use exclusively the first approach. The second approach produces local plans by using local sensor information to avoid obstacles. These methods have received different names: collision avoidance methods, local planners or navigation methods. Obviously, a local plan is a solution to a local scale problem and needs to be integrated into a global planner or with some global information to guarantee the existence of a solution to the global problem.

In order to navigate in complex environments, an autonomous mobile robot needs to reach a compromise between the need for reacting to unexpected events and the need for having efficient and optimized trajectories. Usually, path-planning methods work in two steps: in the first one, a global path in a previous map is calculated, and in the second step, the robot reads the sensor data and the local trajectory is modified in a reactive way. That provides the path-adaptation mechanism to cope with unexpected obstacles or dynamic environments. These methods calculate the global trajectory off-line in an *a priori* known map and the local modifications are made continuously based on the sensor data while the robot is moving.

The reason for using a two-level planning approach is due to the high computational cost required in most motion-planning techniques to achieve an updated environment model and to plan a smooth and dynamically adapted trajectory. The use of a two-level planner strategy decreases the computational cost due to the fact that the global planner is activated occasionally (it can be done off-line) and the local planner, which is much faster, runs on-line. This two-level approach affects the control architecture of the mobile robot. The first mobile robots were based on a sense-model-plan scheme and led to what is referred to in the literature as planned architectures.[1] These architectures present some difficulties in providing fast responses to environmental changes. Posteriorly reactive architectures[2] not only show the advantages of using fast response methods based on a sensor-decision-action scheme to react to environmental changes, but also show the difficulty of extending the reactivity to upper levels. Finally, hybrid deliberative/reactive architectures[3–8] have emerged as a result of the recognition of the advantages provided by planning at high control levels and the advantages provided by reactive architectures at lower control levels.

The Voronoi fast marching method is based on a *sensor-based global path-planning* paradigm. This is a planning approach based on a fast sense-model-plan scheme able to integrate sensor information in a simple grid-based

* Corresponding author. E-mail: moreno@ing.uc3m.es.

https://doi.org/10.1017/S0263574707003384 Published online by Cambridge University Press

environment model and calculate a globally consistent, smooth and safe trajectory which is fast enough to be used as a reactive navigation method. This approach presents some advantages. One is the ability of global planning methodologies to guarantee a path between a given point and the goal point, if one exists. And the other is the smoothness and safety of the solution obtained. This solution eliminates the local minima trap problem and the oscillations in narrow places present in other methods, and also indirectly eliminates the use of a supervision system able to detect local minima failures (obstructed paths) in order to initiate the search for a new and feasible global path from the current position to the goal point.

In order to calculate the trajectory, the proposed method combines the Voronoi extended transform and the fast marching method. The Voronoi approach to path planning has the advantage of providing the safest trajectories in terms of distance to obstacles; but, because its nature is purely geometric, it does not achieve sufficient smoothness. On the other hand, the fast marching method has been applied to path planning,[9] and their trajectories are of minimal distance, but they are not very safe because the path is too close to obstacles and what is more important, the path is not smooth enough. In order to improve the safety of the trajectories calculated by the fast marching method, two solutions are possible: the first possibility, in order to avoid unrealistic trajectories produced when the areas are narrower than the robot, is to eliminate the segments with distances to the obstacles and walls less than half the size of the robot which need to be removed from the Voronoi diagram. The second possibility, used in this paper, is to dilate the objects and walls in a safety distance that ensures the robot does not collide and does not accept passages narrower than the robot size. The last step calculates the trajectory in the image generated by the potential slowness function made by Voronoi extended transform using the fast marching method. In this context, the slowness is proportional to the inverse of the velocity (refractive index in optics). This method creates a funnel potential function that represents a wave expansion with time like the last axis, and in this potential, it looks for a minimum time path by using the gradient method. Then, the path obtained verifies the smoothness and safety considerations required for mobile robot path planning. The advantages of this method are the easy implementation, the speed of the method and the quality of the trajectories. The method works in 2D and 3D, and can be used on a global or local scale, in this case operating only with sensor information instead of using an *a priori* map (sensor-based planning).

The paper is organized as follows. After discussing the related work in Section 2, Section 3 explains the requirements and basic ideas of the method, and in Sections 4–6, the theoretical background of the different ideas used in the method are explained. Section 7 shows some results of the method for an holonomic mobile base. Sections 8 and 9 discuss the contributions of the method with respect to other methods, and contain the conclusions.

## 2. Related Work

The objective of this work is to calculate collision-free trajectories for a mobile robot operating in environments with unknown obstacles (dynamic or not). The technique proposed here avoids the classical partition in *global* and based on *a priori* information (motion planning), and *local* and based on *sensory information* (reactive navigation, collision avoidance or sensor-based local planning).

From a theoretical point of view, the motion-planning problem is well understood and formulated, and there is a set of classical solutions capable of computing a geometrical trajectory that avoids all known obstacles. Mobile robot path-planning approaches can be divided into five classes (according to Latombe[10]). *Roadmap* methods extract a network representation of the environment, and then, apply graph search algorithms to find a path. *Exact cell decomposition* methods construct non-overlapping regions that cover free space and encode cell connectivity in a graph. *Approximate cell decomposition* is similar, but cells are of predefined shape (e.g., rectangles) and do not exactly cover free space. *Potential field* methods differ from the other four ones in that they consider the robot as a point evolving under the influence of forces that attract it to the goal while pushing it away from obstacles. *Navigation functions* are commonly considered a special case of potential fields. Most of these general methods are not applicable if the environment is dynamic or there are no modeled obstacles. Hence, to avoid the problem of executing an unrealistic geometrical trajectory which can collide with obstacles, obstacle avoidance algorithms have been developed to provide a robust way of coping with the problem.

These methods are based on a *perception–action* process that is repeated periodically at a high rate. The process has two steps: first, the sensory information is collected, and then, a motion command is calculated to avoid collisions while moving the robot toward a given goal location (while maintaining the global plan previously determined).

Because of the fast operation rate of the collision-avoidance algorithms, they can deal robustly with unknown obstacles and dynamic scenarios. However, it is difficult to obtain optimal solutions and to avoid trap situations since they use only local sensory information. This classical approach to motion planning is roughly shown in Fig. 1.

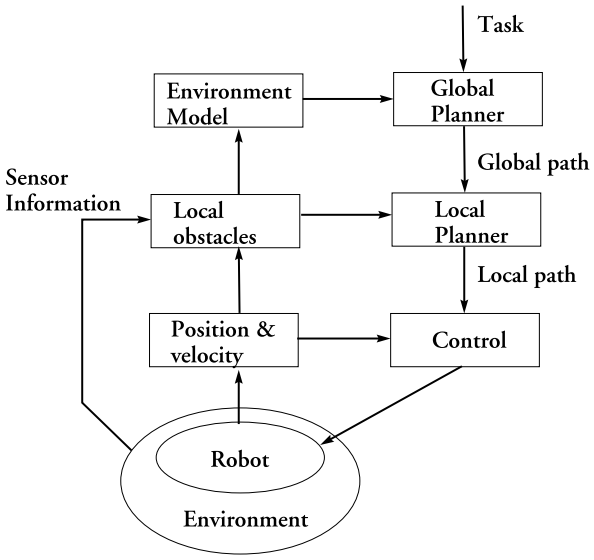



Fig. 1. Classical approach.

https://doi.org/10.1017/S0263574707003384 Published online by Cambridge University Press

Next, we describe some of these related collision avoidance methods.

One of the classical methods for dynamically coping with the collision avoidance problem is the potential field approach developed by Khatib.[11] This approach is based on the creation of an artificial potential field in which the target is an attractive pole and the obstacles are repulsive surfaces. The robot follows the gradient of this potential toward its minimum. This technique can be used at a global or local level depending on the information used to generate the potentials. The major advantage of this method is its simplicity, and the capability of being used dynamically because of the easy treatment of fixed and mobile obstacles. Its major disadvantage is the possible existence of local minima and the oscillations for certain configurations of obstacles. In spite of this problem, this technique has been used extensively in reactive architectures because of its natural ability to encapsulate specific robot behaviors.

A variation of this idea is the vector field histogram (VFH) method proposed by Borenstein and Koren.[12] VFH uses a polar histogram constructed around the robot representing the polar densities of the obstacles. The area with the least density closest to the goal direction is chosen. This technique is simple, but may lead to oscillations and can also be trapped in certain configurations. Posteriorly, VFH+[13] has improved the security distance (object enlarging), reduced oscillations between valleys (hysteresis) and obtained path smoothness. A third version, VFH* has been proposed by Ulrich[14] to include a look-ahead verification of the robot motions in order to avoid local traps. A projected position tree is built by predicting each possible robot movement and searched using A* classic method to choose a motor command.

Among the obstacle avoidance planner (sensor-based local planners), it is possible to find the curvature-velocity method[15] which treats obstacle avoidance as a constrained optimization in velocity space. Vehicle dynamics and obstacle information are converted into constrain and used in the optimization process.

The dynamic window approach[16] also uses a constrained search in the velocity space to determine the convenient speed commands. The use of a grid-based representation makes it simple but increases the memory requirements and the computational cost.

The nearness diagram approach[17] is a situated-activity reasoning system which, based on the sensor information, identifies the situation and determines the corresponding action. It uses a reactive navigation method designed by a symbolic level decision tree which is based on a set of complete and exclusive definitions of the possible situations.

The elastic bands proposed by Quinlan and Khatib[18] represents connected bubbles of the free space subject to repulsive forces from obstacles and attractive forces from neighboring bubbles. The elastic band iteratively smoothes the plan and adapts it to moving or unexpected obstacles.

The majority of these methods have commutation difficulties between the local and the global parts, due to the fact that local avoidance algorithms provide modifications of global trajectories but do not offer solutions when the global trajectory is blocked or trapped in local minima. The classical solution to this problem is to include a supervisor to analyze the global path execution. In case a local trap or a blocked trajectory is detected, it starts a search for a new global path from the current location to the goal point.

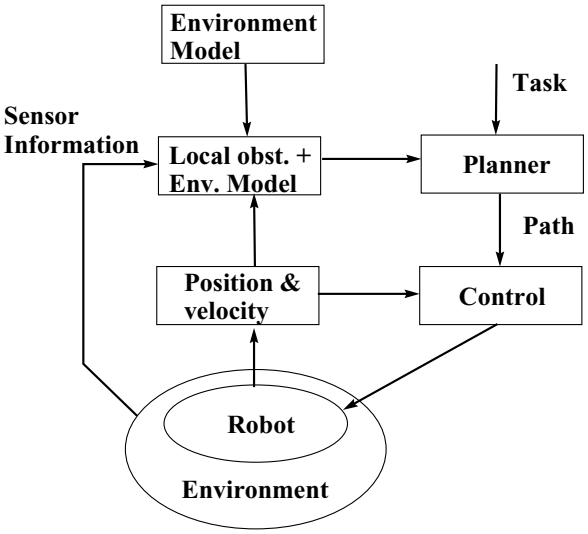



Fig. 2. Sensor-based global planning approach.

The motivation and objective of the present work is to unify the global motion planner and the obstacle avoidance planner in a single planner. This provides smooth and reliable global motion paths which avoid local obstacles from the current position to the goal destination. The motion planning structure with the proposed planner is shown in Fig. 2.

## 3. The Sensor-Based Global Planner Algorithm

The *sensor-based global planner* algorithm proposed in this paper is a potential method, but it does not have the typical problems of the following methods enumerated by Koren and Borenstein:[19]

1) trap situations due to local minima (cyclic behavior),
2) no passage between closely spaced obstacles,
3) oscillations in the presence of obstacles,
4) oscillations in narrow passages.

The proposed method is conceptually close to the navigation functions of Rimon and Koditscheck[20] because the potential field has only one local minimum located at the single goal point. This potential and the paths are smooth (the same as the repulsive potential function) and there are no degenerate critical points in the field. These properties are similar to the properties of the electromagnetic waves propagation in geometrical optics (for monocromatic waves with the approximation that lengthwave is much smaller than the obstacles and without considering reflections or diffractions).

The proposed method has strong physical contents: it consists in the propagation of a wave (like that used in geometrical optics, geometrical acoustics, etc.) from the current position of the robot to the goal, by using a map of slowness (or refractive indexes, or the inverse of velocities) similar to the repulsive electrical potential of walls and obstacles, and the calculation of the path (or light ray in

https://doi.org/10.1017/S0263574707003384 Published online by Cambridge University Press

geometrical optics) by using the gradient method from the goal to the current position point.

The method is based on the following key points:

- *Fast response*: The planner needs to be fast enough to be used reactively in case unexpected obstacles make it necessary to plan a new path. To obtain this fast response, a fast planning algorithm and a fast and simple treatment or modeling of the sensor information are required. A low-complexity-order algorithm is needed to obtain a real-time response to unexpected situations.
- *Smooth trajectory*: The planner must be able to provide a smooth motion plan which can be executed by the robot motion controller. This avoids the need for a local refinement of the trajectory.
- *Reliable trajectory*: The planner will provide a safe (reasonably far from *a priori* and detected obstacles) and reliable trajectory (free from local traps). This avoids the coordination problem between the local avoidance planners and the global planners when local traps or blocked trajectories exist in the environment.
- *Completeness*: As the method consists in the propagation of a wave, if there is a path from the initial position to the objective, the method finds it.

To satisfy all these requirements the sensor-based global planner approach follows these steps:

1) The first step of the algorithm integrates sensor measurements into a grid-based map by updating the corresponding occupied cells. The sensory information is included in the environment map avoiding complex modeling or information fusion. To integrate sensor information, the system must exactly know where the robot is, something that in mobile robotics is more than often not the case. Most mobile robotics research over the past two decades has concentrated not only on trajectory generation, but also on localization and mapping. The authors have proposed an evolutionary filter for robust mobile robot global localization.[21]
2) In a second step, the objects are enlarged in the radius of the mobile robot. This step will eliminate unfeasible paths, and avoid additional path verifications.
3) The updated environment model is then converted into an environment safety image by using the logarithm of the inverse of the Voronoi extended transform in the environment image. This is similar to the electrical repulsive potential of walls and obstacles. In the new image, each position contains the distance to the closest object. That produces a distance map based on the Voronoi extended transform where maxima are obtained just in the Voronoi diagram of the environment model. This enables to know the collision risk of a given trajectory in terms of the distance to obstacles at each point of the trajectory. The step starts with the calculation of the Voronoi diagram of the *a priori* map of the environment (which are the cells located equidistant to the obstacles). This process is done by means of morphological operations on the environment map image.[22,23] To be precise, a skeletonization is done by using image techniques in order to obtain the Voronoi diagram. At the same time, the method calculates the *extended voronoi transform* (EVT) of the map to obtain the Euclidean distances of each cell to the closest obstacle in the environment. This part of the method is also very fast due to the fact that it is done by efficient image-processing techniques. The process has a computational complexity of $O(n)$, as is shown in the work of Yatziv *et al.*[23]. This potential can be interpreted as a slowness map. This slowness is interpreted as the refractive index in optics and acoustics, viscosity in fluid mechanics, etc. The slowness is indicated by the grey level in each point of the image.
4) Based on the slowness map, the fast marching method creates a new potential $T(\mathbf{x})$ that represents the propagation of a electromagnetical wave with the time as third axis in 2D or fourth axis in 3D. This potential is used to calculate the shortest trajectories (in time) based on the potential surface defined by the slowness map. The calculated trajectory is the geodesic in the potential surface, and has a velocity defined in each point. If the fast marching method were used directly on the environment map, we would obtain the shortest geometrical trajectory, but then, the trajectory would be neither safe nor smooth. The method of fast marching solves the eikonal equation that has, by solution, the fastest path that in optics represents the principle of Fermat: *Light travels the path which takes the least time*.

The main reason to separate the trajectory calculation in two parts (in classical approaches) is due to the fact that global path calculation is very slow and it is impossible to recalculate it continuously when the robot is moving. The method proposed here is extremely fast; the whole process (sensing-model-plan) takes only 0.15 s (for a medium length trajectory), letting the algorithm recalculate a path from the current robot's position to the goal location reactively.

## 4. The EVT Transform

In order to get a slowness potential similar to the repulsive electric potential, the EVT is used.

A k-dimensional binary image is a function $I$ from the elements of an $n_1 \times \cdots \times n_k$ array to [0,1]. The elements are called pixels when $n = 2$ and voxels when $n \geq 3$. Voxels of value next to 0 and 1 are called background and foreground or feature voxels, respectively. For a given distance metric, the EVT (also called image distance transform) of an image $I$ is an assignment to each voxel $x$ of the distance between $x$ and the closest feature voxel in $I$, i.e., it consists of associate grey levels for each cell. As a result of this process, a kind of potential proportional to the distance to the nearest obstacles for each cell is obtained. Zero potential indicates that a given cell is part of an obstacle and maxima potential cells correspond to cells located in the Voronoi diagrams (which are the cells located equidistant to the obstacles). This function introduces a potential similar to a repulsive electric potential.

At each dimension level, the transform is computed by constructing the intersection of the Voronoi diagram whose sites are the feature voxels with each row of the image. This construct is performed efficiently by using the transform in the next lower dimension.

https://doi.org/10.1017/S0263574707003384 Published online by Cambridge University Press

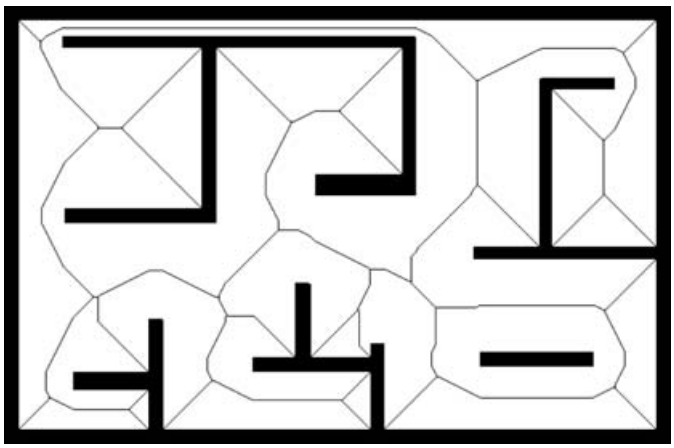


Fig. 3. Map of the room with the Voronoi made by skeletonization.



Fig. 4. Potential of the EVT (slowness map).

The algorithm calculates the Voronoi and the EVT at the same time as can be seen in Fig. 3 (Voronoi diagram) and 4 (EVT). The algorithm used[24] for a $k$-dimensional binary image is linear in the total number of voxels $N$, i.e., it has an $O(N)$ computational complexity. A parallel version of the algorithm runs in $O(N/p)$ time with $p$ processors.

*4.1. Implementation of a smooth slowness function*

This implementation starts with the calculation of the logarithm of the inverse of the EVT of the 2D updated map (*a priori* + sensor data) of the environment (or the inverse of the EVT in case of 3D maps). Each white point of the initial image (which represents free cells in the map) is associated to a grey level that is the logarithm of the inverse of the 2D distance to nearest obstacles. As a result of this process, a kind of potential is obtained, proportional to the distance to the nearest obstacles to each cell, as can be seen in Fig. 4.

This function introduces a potential similar to a repulsive electric potential (in 2D), that can be expressed by

$$\phi = c_1' \log(1/r) + c_2'. \tag{1}$$

If $n > 2$, the potential is

$$\phi = \frac{c_3}{r^{n-2}} + c_4. \tag{2}$$

More precisely, the equation of the electric potential $\phi$ in a region $\Omega$ free of charge with border $\partial\Omega$ and constant potential at obstacles (Dirichlet conditions) is the Laplace equation:

$$\nabla^2 \phi = 0. \tag{3}$$

The solutions of this equation are called harmonic functions. In case of spherical symmetry, the solution depends only on $r$ (distance from the origin). The general expression of the Laplace's equation in polar coordinates can be written as

$$\nabla^2 \phi = \phi_{rr} + \frac{n-1}{r}\phi_r + \text{angular terms}, \tag{4}$$

where $\phi_{rr}$ is the second partial derivative of $\phi$ with respect to $r$ and $\phi_r$ is the first partial derivative with respect to $r$. Since $\phi = \phi(r)$, the angular terms become zero. Then the Laplace equation becomes

$$\phi_{rr} + \frac{n-1}{r}\phi_r = 0 \quad \text{or} \quad \frac{\phi_{rr}}{\phi_r} + \frac{n-1}{r} = 0.$$

Integrating once, we obtain $\phi_r = c_1/r^{n-1}$.

For $n = 2$, the solution is $\phi = c_1 \log(r) + c_2$, as $c_1$ is negative, it is better to write it as

$$\phi = c_1' \log(1/r) + c_2'. \tag{5}$$

If $n > 2$, the solution is

$$\phi = \frac{c_3}{r^{n-2}} + c_4. \tag{6}$$

This result connects the potential defined previously (with the logarithm of the inverse of the EVT) to the harmonic functions, which are the solutions of the Laplace's equation. As can be seen in Eq. (5), the log of the inverse of the EVT (distance) can be calculated as $\phi = c_1' \log(1/r) + c_2$, where $c_1'$ is a positive constant.

## 5. Fundaments of the Method

The laws that govern the propagation of the electromagnetic waves are the Maxwell's laws. To study the transmission of rays, some approach is necessary; a possible approach is the "almost flat waves" (i.e., the optical wave propagates at wavelengths much smaller than image objects so that ray optics can approximate wave optics) in isotropic and possibly non-homogeneous media for a monochromatic wave. These equations, along with the mentioned approach, allow us to develop the theories based on rays such as the geometric optics, the theory of sound waves, etc. Of these equations, the eikonal equation is deduced. In the Sethian[25] notation

$$|\nabla T| F = 1, \tag{7}$$

where $T(\mathbf{x})$ represents the wavefront (time), $F(\mathbf{x})$ is the velocity index of the medium and $\mathbf{x} = (x, y)$ in 2D or $\mathbf{x} = (x, y, z)$ in 3D. In geometrical optics, Fermat's *least*

https://doi.org/10.1017/S0263574707003384 Published online by Cambridge University Press

*time principle* for light propagation in a medium with space-varying refractive index $\eta(\mathbf{x})$ is equivalent to the eikonal equation and it can be written as $||\nabla\Phi(\mathbf{x})|| = \eta(\mathbf{x})$, where the eikonal $\Phi(\mathbf{x})$ is a scalar function whose isolevel contours are normal to the light rays, and the refractive index is the quotient of the speed of the light in the vacuum and the speed of light in the medium whose index calculates. This equation is also known as fundamental equation of the geometrical optics.

The eikonal (from the Greek "eikon," which means "image") is the phase function in a situation for which the phase and amplitude are slowly varying functions of position. Constant values of the eikonal represent surfaces of constant phase, or wavefronts. The normals to these surfaces are rays (the paths of energy flux). Thus, the eikonal equation gives a method for "ray tracing" in a medium of slowly varying index of refractive (or the equivalent for other kinds of waves).

The most important aspect in this equation, from the path planning point of view, is that the solution is an exponential in which the refractive index $\eta$ of the medium appears in the exponent

$$\mathbf{E}(\mathbf{x}, t) = \mathbf{A}(\mathbf{x})\, \mathrm{e}^{i(\Phi(\mathbf{x})-\omega t)},$$

where $\eta(\mathbf{x}) = \omega(\mathbf{x})/\omega_0$. (In the fast marching method, only the propagation of the first arrival of the wave is considered and there are no reflexions, interferences or diffractions, and in our work, there is only one starting point.) As the refractive index is proportional to the slowness of the wave's transmission in the media, the path will be the same function class as the field of slowness. In the nature, the electric field is a sum of terms of the form $\phi = c_1' \log(1/r) + c_2'$ (in 2D) or $E = Kq/r^2$ (in 3D) that is of infinite class whenever we are not upon the charges.

The physical meaning of the eikonal solution is deduced of the classic theory of Hamilton–Jacobi. The eikonal equation can be generalized as

$$\sum_{i,j} a_{ij}(\mathbf{x}) \frac{\partial T}{\partial x_i} \frac{\partial T}{\partial x_j} = 1, \tag{8}$$

where $\mathbf{x} = (x_1, x_2, \ldots)$ is the vector of the coordinates from the space and the coefficients $a_{ij}$ form a defined positive matrix $A$. This equation defines the surfaces characteristics $t = T(\mathbf{x})$ of an hyperbolic linear equation

$$\sum_{i,j} a_{ij}(\mathbf{x}) \frac{\partial^2 u}{\partial x_i \partial x_j} + F\left(\mathbf{x}, u, \frac{\partial u}{\partial x_i}\right) = \frac{\partial^2 u}{\partial t^2}. \tag{9}$$

A well-known theorem (Smirnov, 1964) establishes that the rays of propagation or characteristics of Eq. 8 are the geodesics in the Riemannian metric $\mathrm{d}T = \sqrt{\sum_{i,j} b_i(\mathbf{x})\, \mathrm{d}x_i\, \mathrm{d}x_j}$, where $b_{i,j}$ are the components of the matrix $B = A^{-1}$. For the eikonal isotropic equation, this metric is reduced to the traveltime measure $\mathrm{d}T = s(\mathbf{x})\, \mathrm{d}\sigma$ where $\mathrm{d}\sigma = \sqrt{\sum_i \mathrm{d}x_i^2}$ is the Euclidean metric distance. *In this case, the geodesics are the same as the rays of the Fermat's principle.*

## 6. Intuitive Introduction of the Eikonal Equation and the Fast Marching Planning Method

The propagation of fronts is present in a great variety of situations from the propagation of a wave to the evolution of flames in combustion or the expansion of an oil spill in the sea. Other applications have not been initially confronted, such as movement of interfaces, but can be approached from that point of view, which includes problems in fluid mechanics, combustion, manufacturing of computer chips, computer animation, image processing, structure of snowflakes and the shape of soap bubbles.

The theory and the numerical techniques known as fast marching methods is derived to describe the movement of interfaces, based on a resolution of the equations on partial differential equations as a boundary conditions problem. They have the merit of unifying the ideas relative to the evolution of fronts in a general framework. We will follow Sethian notation.[9]

We introduce the formulation of a front in evolution, having considered a generic limit, for example, an unidimensional expansion, one curve in two dimensions (see Fig. 5) or one surface in three dimensions that separates a region from another.

Let us imagine that the curve or surface moves in its normal direction with a known speed $F$. The objective would be to follow the movement of the interface while this one evolves. A large part of the challenge, in the problems modeled as fronts in evolution, consist of defining a suitable speed, which faithfully represents the physical system.

A way to characterize the position of a front in expansion is to compute the time of arrival $T$, in which the front reaches each point of the underlying mathematical space of the interface. It is evident that for one dimension (see Fig. 6), we can obtain the equation for the arrival function $T$ in an

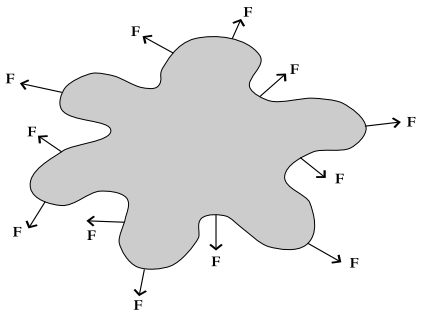



Fig. 5. Wavefront propagating with velocity $F$.

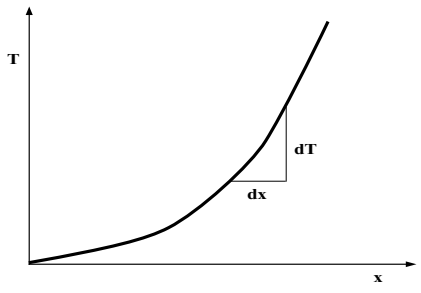



Fig. 6. Formulation of the arrival function $T(x)$, for an unidimensional wavefront.

https://doi.org/10.1017/S0263574707003384 Published online by Cambridge University Press

easy way, simply considering the fact that the distance $x$ is the product of the speed $F$ and the time $T$.

$$x = FT.$$

The spatial derivative of the solution function becomes the gradient

$$1 = F\frac{\mathrm{d}T}{\mathrm{d}x},$$

and therefore, we have that the magnitude of the gradient of the arrival function $T(\theta)$ is inversely proportional to speed

$$\frac{1}{F} = |\nabla T|\,.$$

For multiple dimensions, the same concept is valid because the gradient is orthogonal to the level sets of the arrival function $T(x)$. In this way, we can characterize the movement of the front as the solution of a boundary conditions problem. If speed $F$ depends only on the position, then the equation $1/F = |\nabla T|$ can be reformulated as the eikonal equation

$$|\nabla T|\, F = 1. \tag{10}$$

As a simple example, we defined a circular front

$$\gamma_t = \{(x, y)/T(x, y) = t\}$$

for two dimensions that advance with unitary speed. The evolution of the value of the arrival function $T(\theta)$ can be seen as time goes by (i.e., $T = 0$, $T = 1$, $T = 2$, ...), and the arrival function comes to points of the plane in more external regions of the surface as can be seen in Fig. 7. The condition of contour is that the value of the wave front is null in the initial curve.

The direct use of the fast marching method does not guarantee a smooth and safe trajectory. Due to the way the front wave is propagated, the shortest geometrical path is determined. This makes the trajectory unsafe because it touches the corners, walls and obstacles, as is shown in Fig. 8. This problem can be easily solved by enlarging the obstacles, but even in that case, the trajectory tends to go close to the walls and it is not sufficiently smooth and safe enough.

The use of the EVT together with the fast marching method improves the quality of the calculated trajectory considerably.

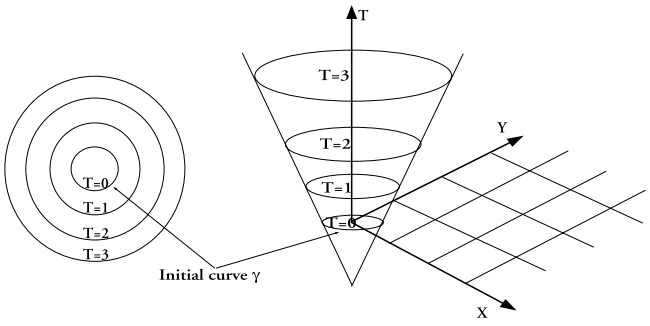



Fig. 7. Movement of a circular wavefront, as a problem of boundary conditions.

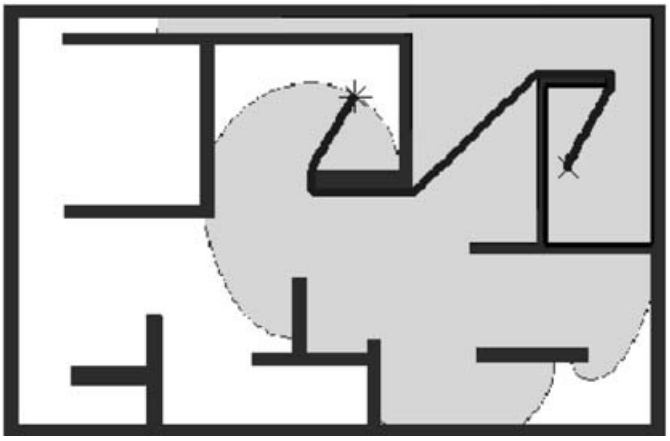


Fig. 8. Trajectory calculated by fast marching method directly, without the use of the EVT.

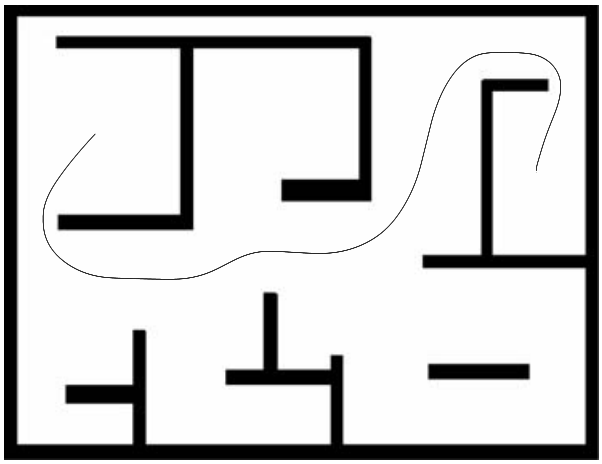


Fig. 9. Trajectory calculated with fast marching with the EVT.

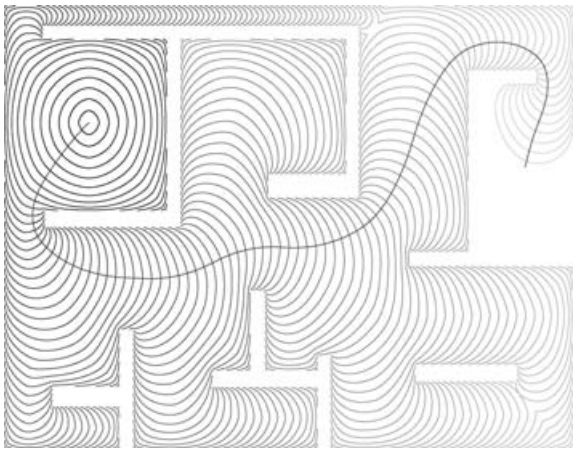


Fig. 10. Front propagation and trajectory of the fast marching method with the EVT.

On one hand, the trajectories tend to go close to the Voronoi skeleton because of the optimal conditions of this area for robot motion, and on the other hand, the trajectories are also considerably smoot. This can be observed in Fig. 9, where the good safe and smooth qualities of the trajectory obtained can be noted. For this environment, in Fig. 10, the isotime level curves with the trajectory can be seen and also that the

https://doi.org/10.1017/S0263574707003384 Published online by Cambridge University Press

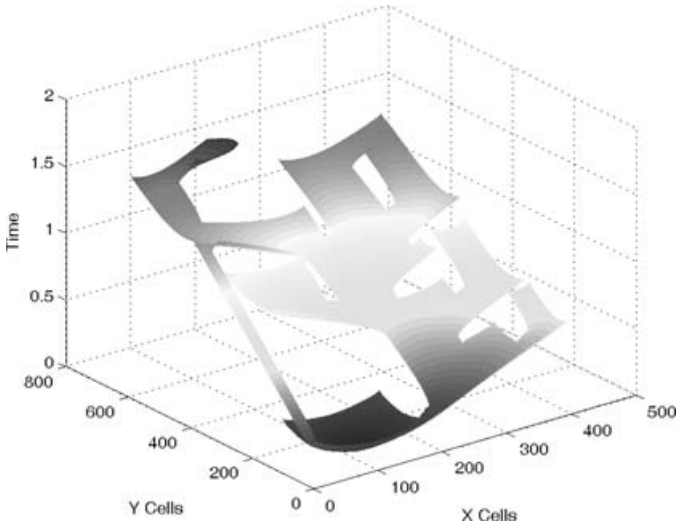



Fig. 11. Potential field of the fast marching method with the EVT.

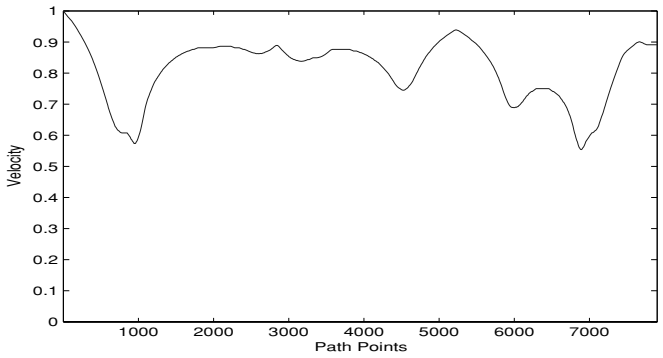



Fig. 12. Velocity of the trajectory of the fast marching method with the EVT.

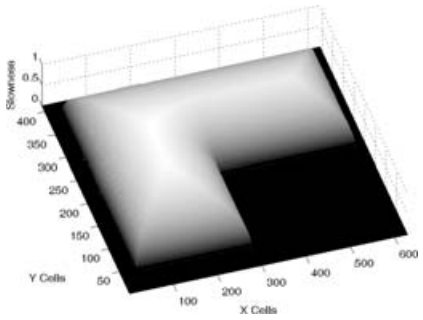



Fig. 13. The EVT applied to an L-shaped environment gives the slowness potential.

trajectory is perpendicular to the level curves. In Fig. 11, the potential field $T(x)$ of the wave propagation is shown. Figure 12 shows the velocity profile reference obtained for the same trajectory made by the slowness map of the EVT of Fig. 4. For a small and easy L-shaped environment, the EVT in 3D is shown in Fig. 13 and the funnel-shaped potential given by the wave propagation of the fast marching method and the path trajectory calculated by gradient method is shown in Fig. 14.

Summing up, the central mathematical idea is to view the moving front $\gamma_t$ as the zero level set of the higher dimensional

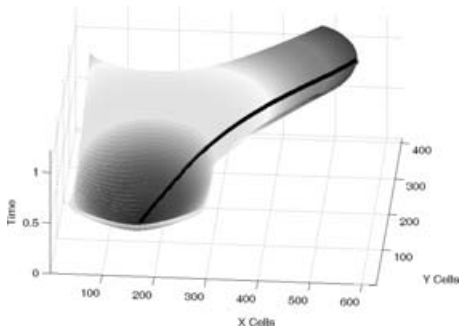



Fig. 14. Funnel-shaped potential of the fast marching method applied to an L-shaped environment and the path calculated with the gradient method.

level set function $\Phi(\mathbf{x}; t)$. Depending on the form of the speed function $V(\mathbf{x})$, the propagation of the level set function $\Phi(\mathbf{x}; t)$ is described by the initial problem for a nonlinear Hamilton–Jacobi type partial differential equation of first or second order.

If $V > 0$ or $V < 0$, it is also possible to formulate the problem in terms of a time function $T(\mathbf{x})$ which solves a boundary value problem for a stationary eikonal equation.

*Fast marching methods* are designed for problems in which the speed function never changes its sign so that the front is always moving forward or backward. This allows us to convert the problem to a stationary formulation, because the front crosses each grid point only once. This conversion to a stationary formulation, in addition to a whole set of numerical solutions, gives it its tremendous speed.

After its introduction, the fast marching method approach has been successfully applied to a wide array of problems that arise in geometry, mechanics, computer vision and manufacturing processes (see ref. [26] for details). Numerous advances have been made in the original technique, including the adaptive narrow band methodology[27] and the fast marching method for solving the static eikonal equation.[9,26] For further details and summaries of level set and fast marching techniques for numerical purposes, see ref. [26]. The fast marching method is an $O(n)$ algorithm as has been demonstrated by Yatziv.[23]

## 7. Results

To illustrate the capability of the proposed method, three test situations are shown. In the first test, the method proposed is applied directly to the data obtained from a laser scan around the robot (Fig. 15), and it can be noted how the method obtains a good tradeoff between trajectory distance, distances to obstacles and smooth changes in the trajectory (Fig. 16).

In a second test, to show global plan capabilities, the method is applied to the whole floor of the building where our laboratory is located. The laboratory plant is around 2000 square meters (medium size). The results are shown in Figs. 17 and 18.

The last test shows the combination of the global and local properties of the method are simulated. In this case, a simple trajectory motion is determined from an initial position to

https://doi.org/10.1017/S0263574707003384 Published online by Cambridge University Press

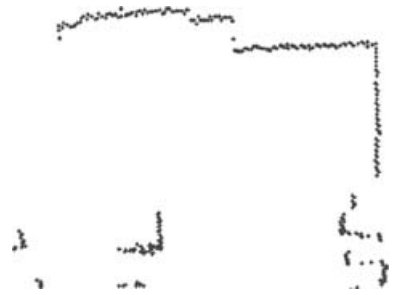


Fig. 15. Laser scan raw data.

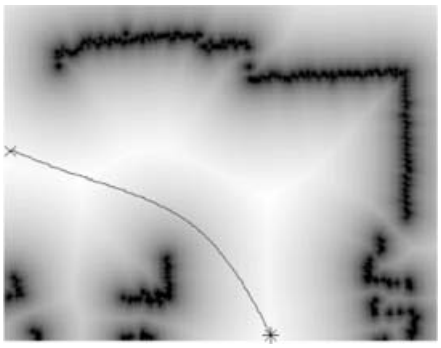


Fig. 16. EVT of the scanned data and trajectory obtained with the fast marching method.



Fig. 17. EVT of the UC3M Robotics Lab plant.

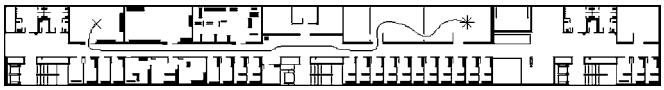


Fig. 18. Motion trajectory obtained with the extended fast marching method.

the goal position. During the movement of the robot, it observes the environment with its laser scan, introduces it in the map and plans a new trajectory. Local observations (obstacles located in the middle of the corridor) originate slightly modified trajectories to avoid the detected obstacles (Fig. 19). In the last image in Fig. 19, the obstacles detected blocked the corridor and the sensor-based global planner finds a completely different trajectory. In the simulation, the included noise level has a covariance of 2% of the distance.

This technique shows the advantage of a technique which is not only local, but also global, which combines sensor-based local planning capabilities with global planning capabilities to react to the obstacles very quickly while maintaining reliability in the planned trajectory. The method always finds the solution if it exists.

## 8. Discussion

We present here a discussion regarding other planning approaches, the limitations of the proposed method and the potential effect on mobile robot's control architecture.

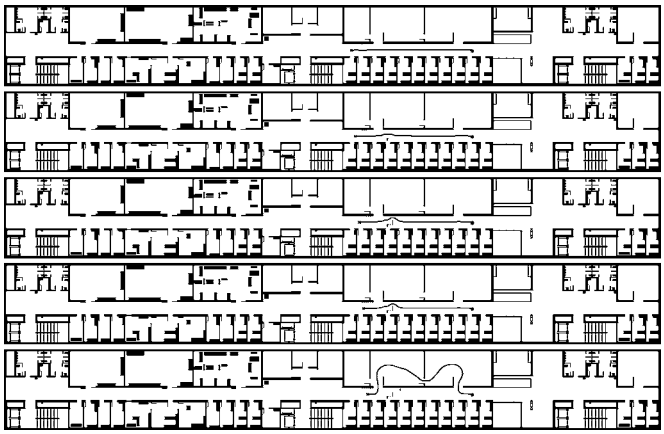


Fig. 19. Dynamic evolution of the path when the robot reads information regarding the new obstacles that are not in the previous map and the robot cannot go along the corridor.

### *8.1. Comparison with existing methods*

The common limitation of all the reactive navigation methods analyzed in this section is that they cannot guarantee global convergence to the goal location because they use only a fraction of the information available (the local sensory information). Some researchers have worked on introducing global information into the reactive collision avoidance methods to avoid local trap situations. This approach has been adopted by Ulrich,[14] who uses a look-ahead verification to analyze the consequences of a given motion a few steps in advance to avoid trap situations. Other authors exploit the information about global environment connectivity to avoid trap situations.[28] Those solutions still maintain the classical two-level approach, and require additional complexity at obstacle avoidance level to improve the reliability at this level.

The Voronoi fast marching is consistent at local and global scale because it guarantees a motion path (if it exists), and does not require global replanning supervision to restart a planning when a local trap is detected or a path is blocked. Furthermore, the path calculated has good safety and smoothness characteristics.

Most of the other methods give paths that are not smooth, even though they only provide a few loose points united by segments of straight lines. The only methods that give comparable results are based on harmonic functions (the solutions of the equation of Laplace) but they have the problem of slowness.

*1) Comparison between the exact navigation methods:* One interesting method that calculates exact navigation functions is the harmonic functions method. Harmonic functions provide optimal potential maps for robot navigation in the sense of minimum length over the potential surface and they are the solutions of the Laplace equation $\nabla^2\Phi(x) = 0$. It has been implemented by using finite differences by da Silva[29,30] and by using the finite elements method (FEM) by Moreno 31 with a high level (usually 1) of the contour conditions for walls and obstacles and a low level (usually 0) for objective. The finite differences method has been used to solve Laplace's equation with the successive over-relaxation (SOR) method, that is an iterative method, and for

https://doi.org/10.1017/S0263574707003384 Published online by Cambridge University Press

Table I. Comparison between the exact navigation methods.

| Method | L (100 × 100) | Room (628 × 412) | Lab. (966 × 120) |
|---|---|---|---|
| SOR (Fc = 1E − 3) | 1.72 s | 164.83 s | 55.58 s |
| SOR (Fc = 1E − 4) | 1.7 s | 191.8 s | 61.38 s |
| Finite elements | 1.34 s | 33.66 s | 16.12 s |
| EVT + FMM | 0.01 s | 0.20 s | 0.15 s |

this reason, it is slow. The FEMs is particularly useful when a robust approximation is sought to solve partial differential equations on a non-homogeneous mesh. Solid mathematical foundations and a great deal of generality allow for different implementations. In Table I, a comparison between the different exact navigation methods is shown. This table compares the SOR method with two different precisions (in this method, the algorithm loops until the desired fractional change (Fc) per iteration is obtained), the FEM and the proposed Voronoi fast marching method (EVT + FMM). As can be seen, the difference of this method with the others in time is very important.

Essential elements and accessory aspects in this method are the following:

- The repulsive potential of walls and obstacles are essential, but there are alternatives to the Voronoi extended transform. Any method that creates a sufficiently smooth potential can be valid if it is sufficiently fast.
- The eikonal equation is essential because it provides a wavefront that expands from a point and creates a new potential in a funnel form in which the minimum time path can be found later. However, the eikonal equation can be solved of many other forms. For example, the equation has been solved by means of finite differences, variational methods by Fomel[32] and other methods such as the fast sweeping method of Zhao.[33] The path can also be calculated by other methods than the gradient method.

The granularity limitation of the method is not due to the slowness potential map nor the wavefront expansion potential nor the least time path calculation over this potential. There are two levels of granularity in the method: the first one is limited by the laser scan frequency because the laser measures are used as raw data, without any kind of time-consuming processing and the second one with a smaller grain by the fast marching method that works with a fine rectangular or triangular grid. At any rate, the grid grain depends only on the scan frequency.

### *8.2. Method limitations*

The main limitation of the Voronoi fast marching method is its computational complexity and the computational differences between initial and final stages of the task execution. Because the fast marching method is a wave propagation technique, the area explored by the algorithm can be quite different. This causes the algorithm to be faster at the end of the task. In spite of its computational efficiency up to medium size environments, the computational cost increases with the environment size. In our test site, the laboratory plant is around 2000 $m^2$ (medium size) and the worst computation time detected is 150 ms (2.2 GHz Pentium IV processor). This time is acceptable for most applications, but because the algorithm has to operate in a reactive way in the case of larger environments, the computational cost has to be controlled.

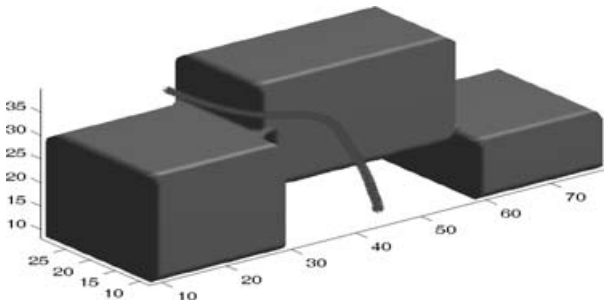



Fig. 20. VFM applied to a 3D problem.

One possible solution is to increase the cell size, and a second solution is to use a multi-resolution map system which uses a large cell size to calculate the motion path in areas outside of a window located around the robot.

The method can be extended to non-holonomic robot structures by modifying the algorithm to operate in the robot configuration space instead of the environment map, but the computational cost increases and its ability to operate in real time decreases.

### *8.3. Architectural effect*

Due to the fact that the Voronoi Fast Marching method integrates global motion planning and obstacle avoidance capabilities in an algorithm, lets us simplify the mobile robot control architecture. This technique has been originally designed for mobile manipulators which requires a smoother and safer motion plan than mobile robots.

From an architectural point of view, it re-opens an old discussion in the mobile robot research community. Can a planned architecture be as efficient and responsive as a reactive architecture? It is a difficult question, but we think that this sensor-based global planning method can lead us to develop efficient and responsive sensor-based planned architectures and to simplify the current hybrid architectures which operate deliberatively at upper architectural levels and reactively at lower levels.

### *8.4. Extensions to 3D systems*

Figure 20 shows the application of the VFM Method to find a path in 3D. The fast marching method can even work in more dimensions, but the method must undergo the problem of the dimensionality.

## 9. Conclusions

We have addressed here a sensor-based global planner. We have presented a method able to deal simultaneously with global and local planning requirements using a combination of the EVT and the fast marching method. The advantage is that our design is able to provide a smooth and safe motion trajectory, and at the same time, guarantees that the trajectory obtained from the current location to the goal location is free from local traps (with the information available at that moment).

To illustrate its possibilities, the method has been used for planning a trajectory in different situations. In the first case,

https://doi.org/10.1017/S0263574707003384 Published online by Cambridge University Press

operating with sensor information only (in this case only as a local planner). In the second case, working as a global planner by using the *a priori* map only and in the third situation operating as a sensor-based global planner using *a priori* information and sensor information, to replan dynamically the trajectory from the current position to the goal position as soon as sensor information originates changes around the robot. The dimensions of the laboratory environment are $116 \times 14$ m (the cell resolution used in the *a priori* information map is 12 cm). For this environment, the first step (the EVT) takes 0.05 s in a Pentium IV at 2.2 GHz, and the second step (fast marching) takes between 0.05 and 0.15 s depending on the length of the trajectory. For a medium distance trajectory on the map, the value is around 0.10 s.

The proposed method is highly efficient from a computational point of view because it operates directly over a 2D image map (without extracting adjacency maps), and due to the fact that fast marching complexity is $O(n)$ and the EVT complexity is $O(n)$, where $n$ is the number of cells in the environment map.

The main contribution of the method is that it robustly achieves smooth and safe motion plans in dynamic scenarios in real time that can be used at low control levels without an additional smoothing interpolation process. This permits the method to fuse collision avoidance and for global planning to be in only one module which can simplify the control architecture of the mobile robot.

## Acknowledgment

The authors would like to thank the Spanish Government for the funds provided by the MICYT Project DPI2004-00594.

## References

1. A. Meystel, "Planning in a hierarchical nested autonomous control system," *Mobile Robots, SPIE Proc.* **727**, 42–76 (1986).
2. R. Brooks, "A robust layered control system for a mobile robot," *IEEE Trans. Robot. Autom.* **2**(1), 14–23 (1986).
3. R. C. Arkin, "Integrating behavioral, perceptual and world knowledge in reactive navigation," *Robot. Autonomous Syst.* **6**, 105–122 (1990).
4. R. C. Arkin, *Behaviour-Based Robotics* (MIT Press, Cambridge, MA, 1998).
5. R. Alami, R. Chatila, S. Fleury, M. Ghallab and F. Ingrand, "An architecture for autonomy," *Int. J. Robot. Res.* **17**(4), 315–337 (1998).
6. R. Chatila, "Deliberation and reactivity in autonomous mobile robot," *J. Robot. Syst. Autonomous Syst.* **16**, 197–211 (1995).
7. R. Bonasso, D. Kortenkamp, D. Miller and M. Slack, "Experiences with an architecture for intelligent, reactive agents," *Lect. Notes Comput. Sci.* **1037**, 187–202 (1996).
8. K. H. Low, W. K. Leow and M. H. Ang, "A hybrid mobile robot architecture with integrated planning and control," in *Proceedings of the 1st International Conference on Autonomous Agents and Multiagent (AMAS'02)*, Bologna, Italy (2002) pp. 219–226.
9. J. Sethian, *Level Set Methods* (Cambridge University Press, Cambridge, UK, 1996).
10. J.-C. Latombe, *Robot Motion Planning* (Kluwer, Dordrecht, The Netherlands, 1991).
11. O. Khatib, "Real-time obstacle avoidance for manipulators and mobile robots," *Int. J. Robot. Res.* **5**, 90–98 (1986).
12. J. Borenstein and Y. Koren, "The vector field histogram—Fast obstacle avoidance for mobile robots," *IEEE Trans. Robot. Autom.* **7**(3), 278–288 (1991).
13. I. Ulrich and J. Borenstein, "Vfh+: Reliable obstacle avoidance for fast mobile robots," in *Proceedings of the IEEE International Conference on Robotics and Automation*, Leuven, Belgium (1998) pp. 1572–1577.
14. I. Ulrich and J. Borenstein, "Vfh*: Local obstacle avoidance with look-ahead verification," in *Proceedings of the IEEE International Conference on Robotics and Automation*, San Francisco, CA (2000) pp. 2505–2511.
15. R. Simmons, "The curvature-velocity method for local obstacle avoidance," in *Proceedings of the IEEE International Conference on Robotics and Automation*, Minneapolis, MN (1996) pp. 3375–3382.
16. D. Fox, W. Burgard and S. Thrun, "The dynamic window approach to collision avoidance," *IEEE Robot. Autom. Mag.* **4**, 23–33 (1997).
17. J. Minguez and L. Montano, "Nearness diagram navigation: Collision avoidance in troublesome scenarios," *IEEE Trans. Robot. Automat.* **20**, 45–59 (2004).
18. S. Quinlan and O. Khatib, "Elastic bands: Connecting path planning and control," in *Proceedings of the IEEE International Conference on Robotics and Automation*, Atlanta, GA (1993) pp. 802–807.
19. Y. Koren and J. Borenstein, "Potential field methods and their inherent limitations for mobile robot navigation," in *Proceedings of the IEEE International Conference on Robotics and Automation*, Sacramento, CA (1991) pp. 1398–1404.
20. E. Rimon and D. Koditschek, "Exact robot navigation using artificial potential functions," *IEEE Trans. Robot. Autom.* **8**(5), 501–518 (1992).
21. S. L. Moreno, "Evolutionary filter for robust mobile robot global localization," *Robot. Autonomous Syst.* **54**(7), 590–600 (2006).
22. H. Breu, J. Gil, D. Kirkpatrick and M. Werman, "Linear time Euclidean distance transform algorithms," *IEEE Trans. Pattern Anal. Mach. Intell.* **17**(5), 529–533 (1995).
23. L. Yatziv, A. Bartesaghi and G. Sapiro, "A fast o(n) implementation of the fast marching algorithm," *J. Comput. Phys.* **212**, 393–399 (2005).
24. J. C. R. Maurer, R. Qi and V. Raghavan, "A linear time algorithm for computing exact Euclidean distance transforms of binary images in arbitrary dimensions," *J. IEEE Trans. Pattern Anal. Mach. Intell.* **25**(2), 265–270 (2003).
25. J. A. Sethian, "A fast marching level set method for monotonically advancing fronts," *Proc. Natl. Acad. Sci. U.S.A.* **93**(4), 1591–1595 (1996).
26. J. A. Sethian, "Theory, algorithms, and aplications of level set methods for propagating interfaces," *Acta Numerica* (Cambridge University Press, Cambridge, UK, 1996) pp. 309–395.
27. D. Adalsteinsson and J. Sethian, "A fast level set method for propagating interfaces," *J. Comput. Phys.* **118**(2), 269–277 (1995).
28. J. Minguez and L. Montano, "Global nearness diagram navigation," in *Proceedings of the IEEE International Conference on Robotics and Automation*, Seoul, Korea (2001) pp. 33–39.
29. E. Prestes e Silva Jr., P. Engel, M. Trevisan and M. Idiart, "Exploration method using harmonic functions," *J. Robot. Autonomous Syst.* **40**(1), 25–42 (2002).
30. E. Prestes e Silva Jr., P. Engel, M. Trevisan and M. Idiart, "Autonomous learning architecture for environmental mapping," *J. Intell. Robot. Syst.* **39**, 243–263 (2004).
31. S. Garrido and L. Moreno, "Robotic navigation using harmonic functions and finite elements," in *Proceedings of the Intelligent Autonomous System (IAS'9)*, Tokyo, Japan (2006) pp. 94–103.
32. S. Fomel, "A variational formulation of the fast marching eikonal solver," *Stanford Exploration Project, Technical Report* (2000) pp. 455–477.
33. H. Zhao, "A fast sweeping method for eikonal equations," *Math. Comput.* **74**(250), 603–627 (2005).
34. V. I. Smirnov, 1964, A course on higher mathematics: Pergamon Press.

https://doi.org/10.1017/S0263574707003384 Published online by Cambridge University Press